Reprinted from

TECTONOPHYSICS

INTERNATIONAL JOURNAL OF GEOTECTONICS AND THE GEOLOGY AND PHYSICS OF THE INTERIOR OF THE EARTH

Tectonophysics 279 (1997) 149–159

Source-side splitting of S waves from Hindu Kush–Pamir earthquakes

S.C. Schoenecker [a], R.M. Russo [b,*], P.G. Silver [c]

[a] *Department of Physics, Princeton University, Princeton, NJ 08544, USA*
[b] *Laboratoire de Tectonophysique, Université de Montpellier II, place Eugène Bataillon, 34095 Montpellier Cedex 05, France*
[c] *Department of Terrestrial Magnetism, Carnegie Institution of Washington, 5241 Broad Branch Rd., N.W., Washington, DC, 20015, USA*

ELSEVIER

ELSEVIER

Tectonophysics 279 (1997) 149–159

TECTONOPHYSICS

Source-side splitting of S waves from Hindu Kush–Pamir earthquakes

S.C. Schoenecker [a], R.M. Russo [b,*], P.G. Silver [c]

[a] *Department of Physics, Princeton University, Princeton, NJ 08544, USA*

[b] *Laboratoire de Tectonophysique, Université de Montpellier II, place Eugène Bataillon, 34095 Montpellier Cedex 05, France*

[c] *Department of Terrestrial Magnetism, Carnegie Institution of Washington, 5241 Broad Branch Rd., N.W., Washington, DC, 20015, USA*

Abstract

We present eight new measurements of source-side S shear wave splitting parameters derived from 20 earthquakes in the Hindu Kush region. For each event–station pair we corrected for receiver-side splitting in order to isolate the source-side contribution to observed splitting. The receiver correction splitting parameters were taken from published values, but we confirmed these values to ensure their accuracy, when possible, via our own observations of SKS splitting at the stations. For two events we found source-side splitting parameters that were identical within errors after correction for receiver splitting at two distant stations with different receiver splitting parameters. Fast polarization directions, ϕ, vary systematically both geographically along the Hindu Kush and Pamir subducted slabs, and with depth: at around 100 km depth in the transition region between the two slabs, ϕ's trend north; at >200 km depth in the Hindu Kush slab, ϕ's trend east-northeast, approximately parallel to the strike of the slab; one measurement at 120 km depth in the Pamir slab trends within 20° of the local slab strike. Delay times, δt, range from 2.3 to 3.7 s, indicating strong upper mantle deformation and alignment of olivine, and/or long source-side travel paths through the anisotropic medium. We interpret our results in the context of two subducted slabs of opposite dip (Hindu Kush slab dipping north, Pamir slab dipping southeast) and shear and compressional flattening around the two slabs caused by the India–Eurasia collision. Thus, north-trending ϕ's at 100 km depth in the transition zone between the two slabs probably represent shear-alignment of upper mantle olivine along the western boundary of the Indian continental lithosphere, now indenting Eurasia along reactivated Mesozoic sutures such as the Chaman Fault. ENE-trending ϕ's from events deeper in the Hindu Kush slab represent flattening and mantle flow along the slab below 200 km. A similar, horizontal slab-parallel flow or olivine alignment may occur beneath the Pamir slab, on the basis of our one measurement there.

Keywords:

1. Introduction

Shear wave splitting occurs when shear waves traverse a seismically anisotropic medium and are split into orthogonally polarized fast and slow shear waves separated by a characteristic delay time, δt (Ando, 1984; Vinnik et al., 1989a,b; Silver and Chan, 1991; Kaneshima and Silver, 1992; Vinnik and Kind, 1993; Helffrich et al., 1994; McNamara et al., 1994; Russo and Silver, 1994a; Silver and Savage, 1994; Yang et al., 1995; Russo et al., 1996a; Gledhill and Gubbins, 1996; Silver, 1996). In the upper mantle, splitting is due to the lattice preferred

* Corresponding author. Present address: Department of Geological Sciences, Northwestern University, 60208 Evanstown, IL, USA. Phone: +1-847-4917383; fax: +1-847-49188060; e-mail: ray@earth.nwu.edu

PII S0040-1951(97)00130-3

orientation of olivine resulting from deformation of olivine-containing aggregates (Hess, 1964; Guéguen and Nicolas, 1980; Christensen, 1984; Nicolas and Christensen, 1987; Ribe, 1989a,b; Mainprice and Silver, 1993). The fast polarization direction, ϕ, expressed as an azimuth, is parallel to the principal axis of extensional finite strain in the deformed, anisotropic medium. The delay time between fast and slow shear wave arrivals is related to the thickness of the constant anisotropy layers traversed, and to the strength of fabric development within these layers. Thus, measurements of shear wave splitting can be used to deduce the orientation and approximate thickness of the anisotropic mantle strain field beneath regions of interest, like the Hindu Kush, yielding important insight into tectonic processes occurring at depth. In particular, assuming upper mantle fabric development can be approximated by a hexagonally symmetric medium with a horizontal symmetry axis, the directions and relative significance of past and current upper mantle shear and compressional strains can be estimated, and possibly related to surface geology and tectonics.

2. Tectonic setting

The Hindu Kush (HK) and Pamir mountain ranges (Fig. 1) lie at the northwestern edge of the Himalayas, approximately marking the westward termination of the India–Eurasia collision zone (Molnar and Tapponnier, 1975; Tapponnier and Molnar, 1976; Mattauer et al., 1978; Tapponnier et al., 1981; Searle et al., 1987; Dewey et al., 1989). The India–Eurasia collision was preceded by a long period of rapid convergence (Patriat and Achache, 1984; Le Pichon et al., 1992), subduction of Tethyan oceanic lithosphere beneath Eurasia (Searle et al., 1987), and accretion of Gondwana-derived terranes to continental Eurasia along sutured boundaries during the Mesozoic (Tapponnier et al., 1981). Continent–continent collision began sometime between 66 and 55 Ma, and apparently was complete (i.e., no intervening oceanic Tethys at the surface) by 49 Ma (Beck et al., 1995). The current rate of the northward motion of India is around 5 cm/yr (DeMets et al., 1990). The persistence of convergence after the collision was complete has resulted in a strong indentation of the southern limit of continental Eurasia (e.g., Patzelt et al., 1996), and some degree of southwestward extrusion of accreted Eurasia crust immediately west of the India–Eurasia boundary along the western portion of the collision zone. The pre-collision tectonic history of the Hindu Kush–Pamir region is relevant to this study because a number of the suture zones marking boundaries of accreted terranes were reactivated as strike-slip faults during the India–Eurasia collision, and thereby facilitated India's northward indentation and southwestward lateral extrusion (Tapponnier et al., 1981; Treloar and Izatt, 1993). These suture zones also mark the surface projection of the India–Eurasia boundary, and are potentially surface loci where slabs now in the upper mantle beneath the study region were subducted or originally attached. Thus (Fig. 1), the Chaman, Herat, and Panjshir Faults, and the Panjao Suture (all Mesozoic suture zones, marked by occurrence of ophiolites) appear to delimit crustal, and perhaps lithospheric, blocks that are, or were recently, in active relative motion. Shear deformation associated with these motions likely extends vertically through the lithospheres involved and may also affect deeper parts of the upper mantle normally considered to be asthenosphere. The left-lateral Chaman and Panjshir faults are particularly important for our study because they are probably the surface expressions of the western boundary of Indian continental lithosphere at depth.

Subcrustal structure in the study region is delimited by active seismicity (Fig. 2) and a few seismic structure studies. Although crustal thickness is variable, it is generally thicker than normal continental crust (e.g., 50–70 km) as a result of shortening and thickening driven by collision (Brandon and Romanowicz, 1986; Molnar, 1988; Burtman and Molnar, 1993; Mellors et al., 1995). Seismicity down to 75 km is diffuse and patchy (Fig. 2) throughout this crust and uppermost mantle, however, and does not clearly define any active structures (Prevot et al., 1980), although good evidence for both thrust (active crustal shortening) and strike-slip (lateral extrusion and continental transform motions) activity exists (Fan et al., 1994). Intermediate-depth (h>75 km) earthquakes, however, clearly define the presence of subducted lithosphere within the study region (Lukk and Vinnik, 1975; Billington et al., 1977; Chatelain et al., 1980; Roecker et al., 1980; Katok, 1988; Fan et al., 1994). Travel-time inversions for the region

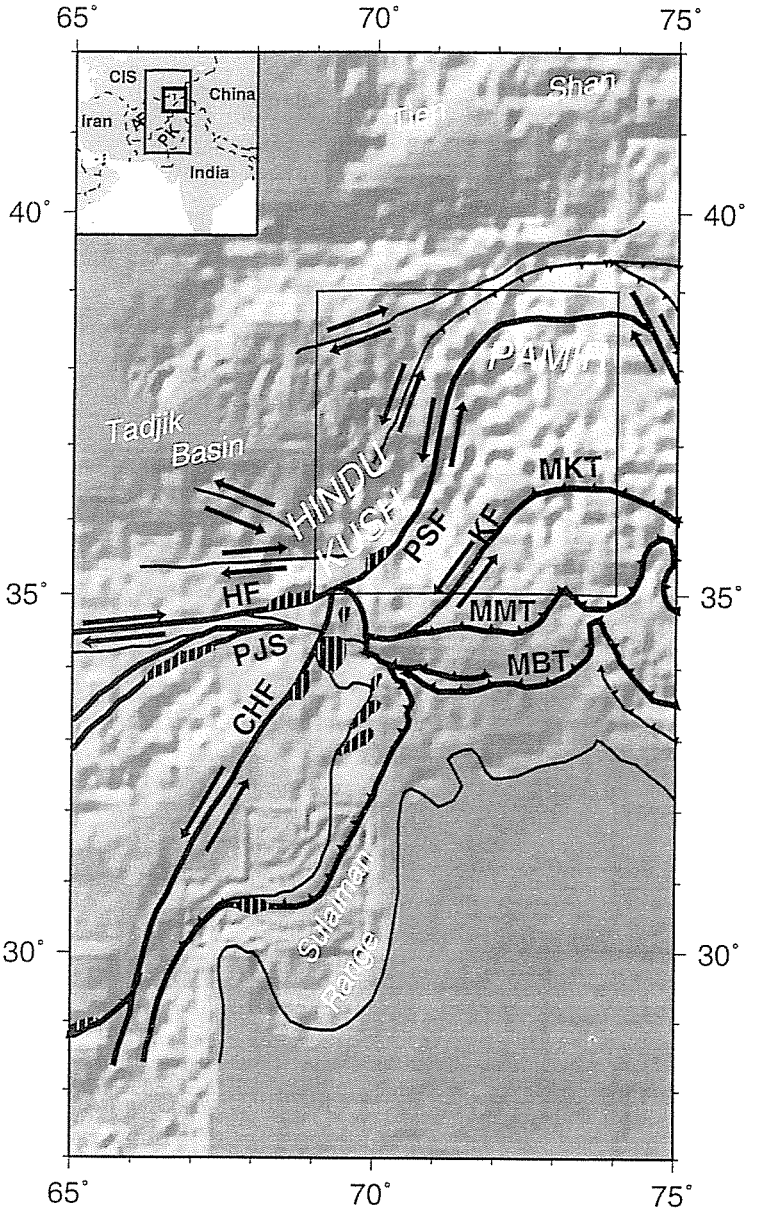

Fig. 1. Map of the Hindu Kush–Pamir study region. Topography is etopo5. Suture zones marking closed oceanic basins and boundaries of terranes accreted to Eurasia in the Mesozoic are shown with heavy lines. Teeth on hanging wall sides of faults. Arrows show senses of recent displacement on strike-slip faults. Box shows area of Figs. 2 and 4. *CHF* = Chaman Fault; *HF* = Herat Fault; *KF* = Kunar Fault; *MBT* = Main Boundary Thrust; *MKT* = Main Karakoram Thrust; *MMT* = Main Mantle Thrust; *PJS* = Panjao Suture; *PSF* = Panjshir Fault. Geology after Tapponnier et al. (1981) and Beck et al. (1995).

reveal a high-velocity slab beneath the Hindu Kush (Mellors et al., 1995) at depths between 200 and 400 km, but Roecker (1982) found evidence for a low-velocity shallow (70–150 km) portion of this Hindu Kush slab. Active seismicity (Billington et al., 1977) and the travel-time inversions indicate an east–west strike and a steep northward dip for the HK slab. Although active seismicity also delineates a north- to

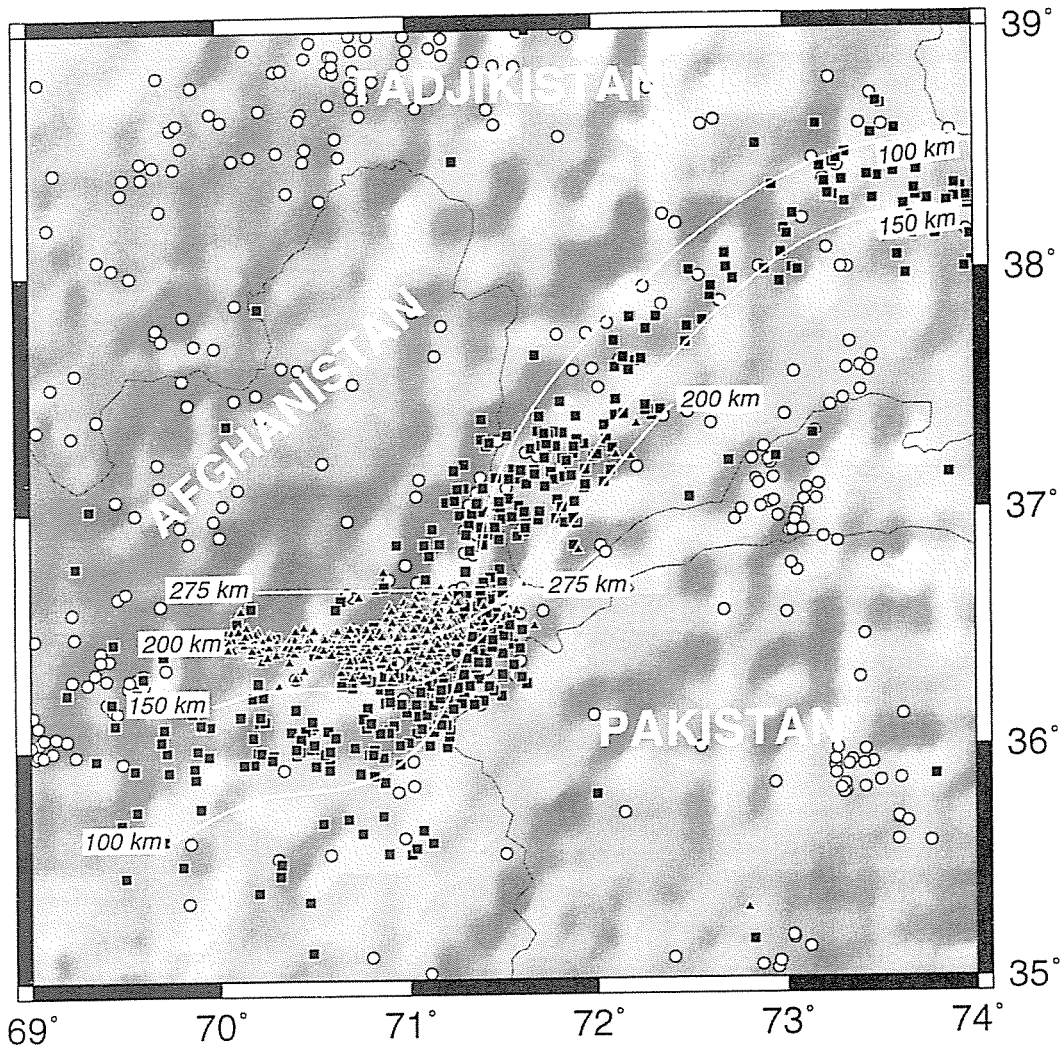

Fig. 2. Seismicity (NEIS, 1963–1995) of the Hindu Kush–Pamir study region. Contours of isodepth to top of subducted lithosphere from Billington et al. (1977). Note that two slabs are present: the Hindu Kush slab striking east and dipping north, and the Pamir slab striking northeast and dipping southeast. Symbols are hypocenters located based on 20 or more stations. White circles: 0–75 km depth; black squares: 75–200 km depth; black triangles: 200–300+ km depth. Topography is etopo5.

northeast-striking, southeastward-dipping Pamir slab extending from 100 km to 200 km depth (Fig. 2; Billington et al., 1977), this slab is not resolved by the tomography studies (Mellors et al., 1995). Thus, although the deep, high-velocity portion of the HK slab has been postulated to be subducted oceanic lithosphere (Mellors et al., 1995), the Pamir slab is apparently different in nature from the deep HK slab. Both the shallow portion of the HK slab and the Pamir slab in its entirety have been interpreted as subducted continental crust (Roecker, 1982; Mattauer, 1983, 1986a,b; Hamburger et al., 1992; Burtman and Molnar, 1993; Fan et al., 1994). Both interpretations (continental subduction and existence of a deep, oceanic HK slab) present problems: continental crust may be too buoyant to subduct to any great depth; and if India–Eurasia collision had proceeded to suturing by 49 Ma (see above), then any Tethyan oceanic lithosphere should have subducted into the lower mantle by now, given continuing convergence during the late Cenozoic. However, the actual nature of the slabs is only marginally important to our work

because in either case the slabs are composed of deforming mantle that is more rigid than the surroundings, and thus the slabs have an important influence on deformation in their environs. It is the nature of this deformation we seek to characterize via the source-side shear wave splitting measurements.

3. Data, method, and measurements

We searched the GDSN, Geoscope, and IRIS digital seismogram archives for the years 1980 to 1994 for earthquakes in the Hindu Kush with body wave magnitudes of 5.6 or greater, depths of at least 40 km (to avoid contamination by surface reflected phases like pS and sS), and that were recorded in the distance range suitable for observing isolated S waves (30° to 82° Δ). A total of 138 individual records with these characteristics from 20 different events were deemed to have an S phase and signal-to-noise ratio of sufficiently high quality to warrant analysis for source-side splitting.

Splitting of teleseismic S waves can occur both in the source event region and in the upper mantle beneath the receiver. Therefore, it is necessary to correct the phases for known receiver-side splitting. The correction requires accurate knowledge of the receiver station splitting parameters; we took station splitting parameters from published studies (Vinnik et al., 1992; Helffrich et al., 1994), but in order to ensure that the correction parameters were good, we carefully checked available data at all the stations, using the method of Silver and Chan (1991) on SKS and SKKS phases recorded at those stations to determine receiver splitting parameters. The station splitting parameters we found for SSB, KONO, and OBN were consistent with published values; however, splitting parameters at GDH and TATO were difficult to constrain accurately. For GDH, we obtained only moderately well-constrained nulls, which although they may indicate an absence of receiver splitting at GDH, do not contradict the published station splitting values of $\phi = -60°$ and $\delta t = 1.2$ s (Vinnik et al., 1992). Fortunately, the GDH correction did not significantly alter the splitting measurement for the single event, 85210, for which we used it, so the source-side fast polarization direction obtained for this event was deemed to be accurate. We obtained no reliable SKS measurements for station TATO, so we could not verify the station correction. For this reason, although the TATO measurement (92339) passes our usual diagnostic tests, the source-side splitting values for the event should be regarded as tentative. This is especially true because the published delay-time correction for TATO is large (Vinnik et al., 1992), and if incorrect, will corrupt the source-side measurements. We then used the method described by Russo and Silver (1994a) to analyze the receiver corrected S phases for source-side splitting.

We obtained eight definite source-side splitting measurements (e.g., Fig. 3), as well as seven well-constrained null measurements (absence of detectable splitting) that were consistent with the positive splitting observations. The eight measurements are listed in Table 1 and plotted at the surface projections of the source event locations on the map in Fig. 4. For two events, we were able to make source-side measurements from seismograms recorded at two receivers, and in each case both measurements were consistent within small errors (Fig. 4, events 85210 and 93221.11), even though the receiver corrections applied were different. The consistency of these results increased our confidence in the reliability of the results in general. Several additional seismograms also showed well-constrained uncorrected splitting, but as no station corrections were available, we excluded them from further consideration since they could not be corrected for potential splitting at the receiver. In addition to the definite splitting measurements, we obtained seven reliable, well-constrained null measurements. Null directions should coincide with the fast or slow polarization directions if anisotropy is present, and this was indeed the case in our study: the null directions are consistent with the splitting measurements when their uncertainties are taken into account. Thus, we take the source-side splitting measurements as an accurate representation of the strain field in the Hindu Kush–Pamir region.

4. Discussion

As shown in Fig. 4, ϕ values appear to fall into two groups: one group (93221.11, 93221.12, and 92339) includes measurements with ϕ's that are approximately locally parallel to adjacent slab contours, and ϕ's of the second group (85210, 89205,

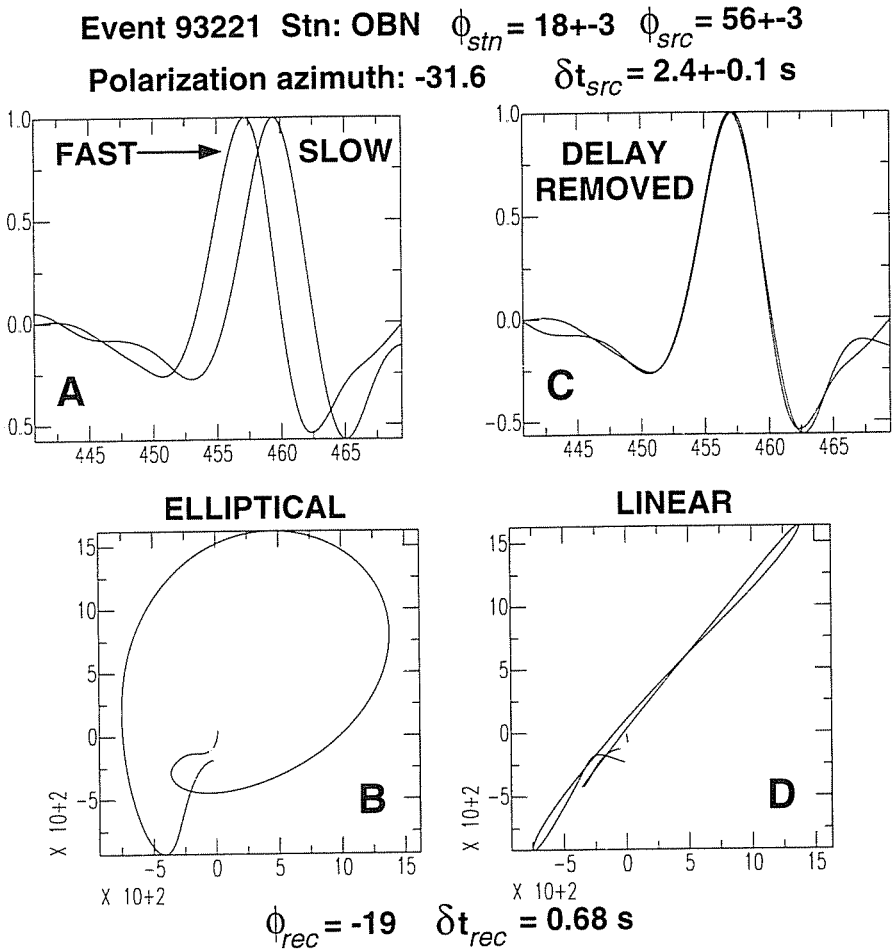

Fig. 3. Example of individual splitting measurements at station OBN for event 93221 (see Table 1). Fast and slow waveforms from measurement window and particle motions. (A) Fast and slow waveforms in the fast and slow reference frame. (B) Same waveforms, delay removed; note excellent waveform coherence. (C) Particle motion of waveforms in upper left frame; note clear ellipticity. (D) Linearized particle motion of delay-removed phases.

Table 1
Splitting parameters

Event	Lat. (degr.)	Long. (degr.)	Depth (km)	Station	Back azimuth (degr.)	ϕ (degr.)	δt (s)
85210	36.168	70.890	101	GDH	341	−2±4	2.8±0.2
85210	36.168	70.890	101	SSB	302	−10±3	3.0±0.4
89205	35.780	71.280	105	SSB	303	9±6	3.5±0.2
90036	37.047	71.250	109	SSB	302	−11±8	2.5±0.3
92339	37.814	72.914	120	TATO	93	18±8	3.7±0.6
93221.11	36.436	70.711	204	KONO	321	62±4	2.3±0.2
93221.11	36.436	70.711	204	OBN	320	55±5	2.4±0.1
93221.12	36.379	70.868	215	KONO	321	64±5	2.6±0.2

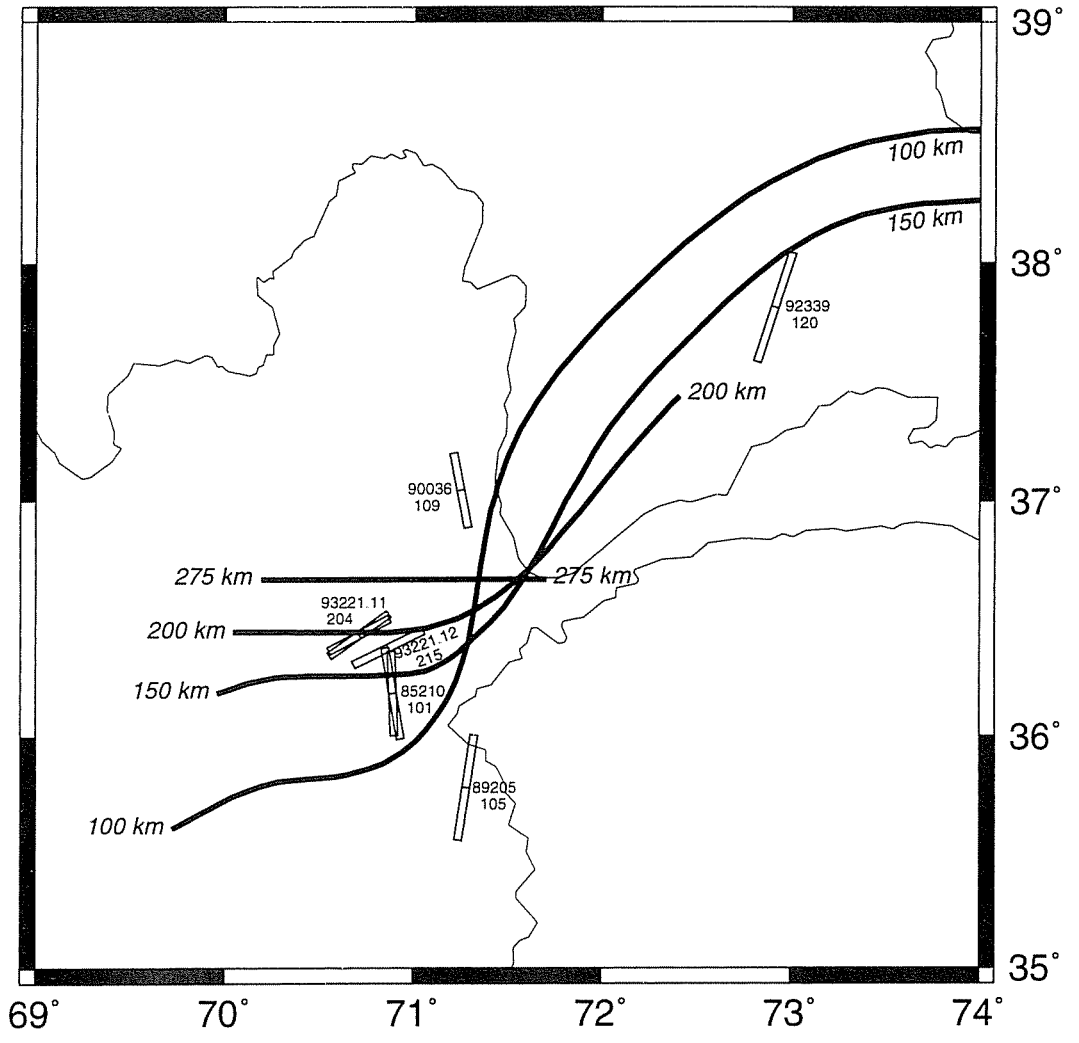

Fig. 4. Map of source-side S splitting measurements. Fast polarization directions, ϕ, are given by azimuth of bars. Event information includes date and hypocentral depth of earthquake: the measurements are projected to the surface. Slab contours from Billington et al. (1977). Note ϕ's are approximately parallel to the local HK slab strike for two events at around 200 km depth, but are at a high angle to local slab strike at 100 km depth.

and 90036) are approximately north-trending. The two events in the slab-parallel group associated with the HK slab occurred at around 200 km depth, and we infer that upper mantle strain along the path from the hypocentral depths to the 410 km discontinuity (base olivine stability field) consists of an along-slab extension, and probably a slab-perpendicular compression (Fig. 5). Although the number of measurements is small, they are very consistent and show no signs of splitting complications that might arise from a complicated anisotropy (e.g., multiple layers: Silver and Savage, 1994; or dipping symmetry axis: Babuška et al., 1993). Thus, the mantle strain field beneath (i.e., on the southern, Indian, side) the HK slab indicates E–W extension and N–S compression at depths of 200–400 km. This interpretation is consistent with the general N–S compressional, E–W extensional strain field observed at the surface, related to India–Eurasia collision (Molnar and Tapponnier, 1975; Tapponnier and Molnar, 1976; Mattauer et al., 1978; Tapponnier et al., 1981; Searle et al., 1987; Dewey et al., 1989). An interesting

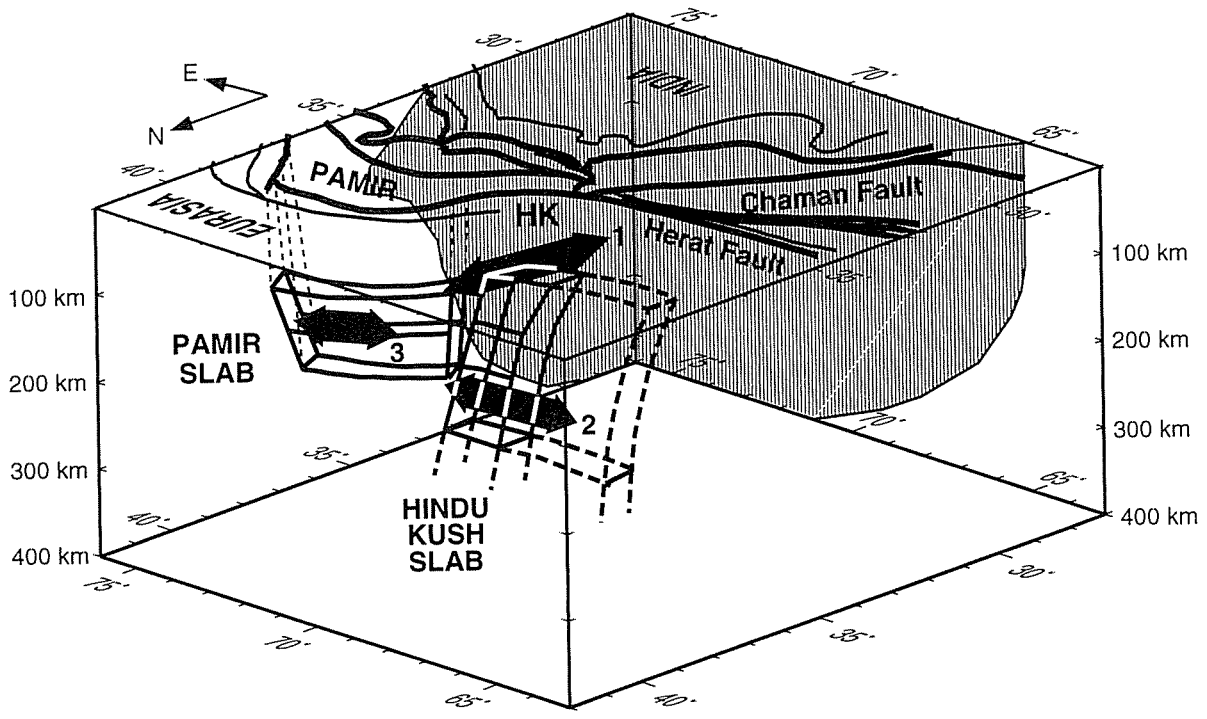

Fig. 5. Block diagram of the study region; view is from NW. Surface sutures as in Fig. 1, positions of slabs derived from Billington et al. (1977): Pamir slab dips southeast, directly away from viewer, HK slab dips north. Three regions of source-side splitting measurements, discussed in text, are shown (large black arrows, numbered): region *1*, shallow (100–200 km) N–S shear zone along which India has indented Eurasia, and which is the interaction zone of the Pamir and HK slabs; region 2, deep (200–400 km) anisotropic zone of E–W extension along the HK slab; region *3*, extension along Pamir slab. Indian continental lithosphere (schematic) in vertical stripe pattern.

inference that can be made from this interpretation is that driving forces of India–Eurasia collision apparently operate, or at least affect mantle strain, at the depth of the strain detectable via the splitting measurements, 200–400 km, in the study region (as well as at shallower levels).

We make a similar interpretation of the one measurement from the Pamir subduction zone (event 92399; Figs. 4 and 5). Because the source-event azimuth is almost due east, but the slab dips southeast, locally, S waves from this event are most likely sampling upper mantle on the north side of the Pamir slab. The sub-slab strain field apparently includes NE extension, and perhaps also NW–SE compression, beneath the Pamir slab. Given the hypocenter depth, the upper mantle strain field indicated by this measurement may extend from 120 km to the 410 km discontinuity. We advance this interpretation tentatively because of the unsubstantiated splitting correction for receiver station TATO.

The second group of splitting measurements (85210, 89205 and 90036) are from events which occurred at around 100 km depth, and which have a general northward ϕ trend that parallels the N–S strike of the Pamir slab in this region, and also the coincident apparent N–S-trending termination of the seismically defined HK slab. The three measurements effectively lie at the interaction boundary between the HK and Pamir slabs, and are parallel to this boundary (Fig. 5). We suggest that they represent upper mantle shear at the western edge of the Indian continental lithosphere that has indented the Eurasian margin here. Surface expressions of this indentation and shear, and of consequent southwestward extrusion of Afghan terranes, include the Panjshir and Chaman faults that approximately overlie the source region of these events. Thus, Indian continental lithosphere, and also intervening terranes, have moved northward on the east side of these shears, and this deformation has affected the mantle

to significant depths: the events were at 100 km, and the shear wave splitting was incurred beneath this depth, but probably above the anisotropic region associated with compression along the deeper HK slab, discussed above (Fig. 5). We note that the shear waves from these events most likely also traversed the deeper deformed HK slab layer, but were not apparently split again by this layer because the two anisotropies are perpendicular (Fig. 4), and thus the deeper symmetry axis is a null direction for the waves already split by the shallower, N–S symmetric medium. Thus, this shear along the western edge of the Indian lithosphere may not extend beneath 200 km depth. The upper mantle strain field thus probably includes tectonically important vertical deformation gradients in this region. The presence of important horizontal gradients in this strain field is indicated by the lack of SKS–SKKS splitting found 100 km or so southeast of our study region by Sandvol et al. (1994).

The delay times we observed in our study, 2.4–3.7 s, are amongst the highest yet observed for source-side splitting measurements (Russo and Silver, 1994a,b; Silver and Russo, 1995; Russo et al., 1996b). However, they are not inconsistent with the anisotropic layer thicknesses mentioned above (200 km for the deeper HK events, 100–300 km for the shallower events), given the likelihood of non-vertical (e.g., longer) travel paths through these anisotropic mantle layers, and with, perhaps, a stronger than normal fabric development (greater intrinsic anisotropy). A stronger mantle fabric might be expected in this region, the site of the most important crustal shortening and thickening on Earth today.

5. Conclusions

We have examined anisotropy in the upper mantle beneath the Hindu Kush by measuring source-side splitting from intermediate-focus events in that region. The eight fast polarization directions we found fall into two groups. In one group, at 200 km in the Hindu Kush slab, ϕ's are locally parallel to the contours of the HK slab; a single measurement from a Pamir slab event also falls in this group. We interpret these splitting measurements as indicating horizontal extension, at depth, along the HK and Pamir slabs, and probably with horizontal compression perpendicular to the slabs. The second group of events, at 100 km depth beneath the western boundary of the Indian continental lithosphere, and along the India–Eurasia interaction zone between the HK and Pamir slabs, have N–S-trending ϕ's. We relate these measurements to shear deformation along this boundary caused by indentation of Eurasia by India, and consequent southwestward extrusion of terranes accreted to Eurasia in the Mesozoic. Both sets of measurements indicate that deformation associated with the India–Eurasia collision and indentation of the Eurasian margin extends throughout the uppermost mantle beneath the study region.

Acknowledgements

Many, many thanks to Adolphe Nicolas for his support and his encouragement of our work these past years. We thank M. Mattauer for helpful discussion of the tectonics of the Hindu Kush–Pamir region. A. Vauchez and an anonymous reviewer provided us with constructive reviews that helped us to greatly improve this paper. We thank Dave Mainprice and Françoise Boudier for their great patience. We used GMT by Wessel and Smith (1991, 1995) to make figures in this paper. This work was supported by NSF grants EAR 93-16457 to P. Silver and R. Russo, and by an NSF–NATO Fellowship to R. Russo.

References

Ando, M., 1984. ScS polarization anisotropy around the Pacific Ocean. J. Phys. Earth 32, 179–196.

Babuška, V., Plomerova, J., Šilený, J., 1993. Models of seismic anisotropy in the deep continental lithosphere. Phys. Earth Planet. Inter. 78, 167–191.

Billington, S., Isacks, B.L., Barazangi, M., 1977. Spatial distribution and focal mechanisms of mantle earthquakes in the Hindu Kush–Pamir region: a contorted Benioff zone. Geology 5, 699–704.

Beck, R.A. et al., 1995. Stratigraphic evidence for an early collision between northwest India and Asia. Nature 373, 55–58.

Brandon, C., Romanowicz, B., 1986. A 'no-lid' zone in the Central Chang-Thang platform of Tibet: evidence from pure path phase velocity measurements of long period Rayleigh waves. J. Geophys. Res. 91, 6547–6564.

Burtman, V.S., Molnar, P., 1993. Geological and geophysical evidence for deep subduction of continental crust beneath the Pamir. Geol. Soc. Am. Spec. Pap. 281, 76.

Chatelain, J.L., Roecker, S.W., Hatzfeld, D., Molnar, P., 1980. Microearthquake seismicity and fault plane solutions in the Hindu Kush region and their tectonic implications. J. Geophys. Res. 85, 1365–1387.

Christensen, N.I., 1984. The magnitude, symmetry and origin of upper mantle anisotropy based on fabric analyses of ultramafic tectonics. Geophys. J.R. Astron. Soc. 76, 89–112.

DeMets, D.C., Gordon, R.G., Argus, D.F., Stein, S., 1990. Current plate motions. Geophys. J. Int. 101, 425–478.

Dewey, J.F., Cande, S., Pitman, W.C., 1989. Tectonic evolution of the India/Eurasia collision zone. Eclogae Geol. Helv. 82, 717–734.

Fan, G., Ni, J.F., Wallace, T.C., 1994. Active tectonics of the Pamirs and Karakorum. J. Geophys. Res. 99, 7131–7160.

Gledhill, K., Gubbins, D., 1996. SKS splitting and the seismic anisotropy of the mantle beneath the Hikurangi subduction zone, New Zealand. Phys. Earth Planet. Inter. 95, 227–236.

Guéguen, Y., Nicolas, A., 1980. Deformation of mantle rocks. Annu. Rev. Earth Planet. Sci. 8, 119–144.

Hamburger, M.W., Sarewitz, D.R., Pavlis, T.L., Popandopulo, G.A., 1992. Structural and seismic evidence for intracontinental subduction in the Peter the First Range, central Asia. Geol. Soc. Am. Bull. 104, 397–408.

Helffrich, G.R., Silver, P.G., Given, H.K., 1994. Shear wave splitting variation over short spatial scales on continents. Geophys. J. Int. 119, 561–573.

Hess, H.H., 1964. Seismic anisotropy of the uppermost mantle under oceans. Nature 203, 629–631.

Kaneshima, S., Silver, P.G., 1992. A search for source side mantle anisotropy. Geophys. Res. Lett. 19, 1049–1052.

Katok, A.P., 1988. On the deepest earthquake in the Pamir–Hindu Kush zone . Izv. Acad. Sci. USSR, Phys. Solid Earth (English transl.) 24, 649–653.

Le Pichon, X., Fournier, M., Jolivet, L., 1992. Kinematics, topography, shortening, and extrusion in the India–Eurasia collision. Tectonics 11, 1085–1098.

Lukk, A.A., Vinnik, L.P., 1975. Tectonic interpretation of the deep structure of the Pamirs. Geotectonics 5, 300–304.

Mainprice, D., Silver, P.G., 1993. Interpretation of SKS-waves using samples from the subcontinental lithosphere. Phys. Earth Planet. Inter. 78, 257–280.

Mattauer, M., 1983. Subduction de lithosphère continentale, décollement croûte–manteau et chevauchements d'échelle crustale dans la chaîne de collision himalayan. C.R. Acad. Sci. Paris 296, 481–486.

Mattauer, M., 1986a. Intracontinental subduction, crust–mantle décollement and crustal stacking wedge in the Himalayas and other collision belts. In: Coward, M.P., Ries, A.C. (Eds.), Collision Tectonics. Geol. Soc. London Spec. Publ. 19, 37–50.

Mattauer, M., 1986b. Les subductions intracontinentales des chaînes tertiaires d'Asie; leurs relations avec les décrochements. Bull. Soc. Geol. Fr. Sér. 8, 2, 143–157.

Mattauer, M., Proust, F., Tapponnier, P., Cassaigneau, C., 1978. Ophiolites, obductions et tectonique globale dans l'est de l'Afghanistan. C.R. Acad. Sci. Paris, Sér. D 287, 983–985.

McNamara, D.E., Owens, T.J., Silver, P.G., Wu, F.T., 1994. Shear wave anisotropy beneath the Tibetan Plateau. J. Geophys. Res. 99, 13655–13665.

Mellors, R.J., Pavlis, G.L., Hamburger, M.W., Al-Shukri, H.J., Lukk, A.A., 1995. Evidence for a high-velocity slab associated with the Hindu Kush seismic zone. J. Geophys. Res. 100, 4067–4078.

Molnar, P., 1988. A review of geophysical constraints on the deep structure of the Tibetan Plateau, the Himalaya, and the Karakoram, and their tectonic implications. Philos. Trans. R. Soc. London A 326, 33–88.

Molnar, P., Tapponnier, P., 1975. Cenozoic tectonics of Asia: effects of a continental collision. Science 189, 419–426.

Nicolas, A., Christensen, N.I., 1987. Formation of anisotropy in upper mantle peridotites — a review. In: Fuchs, K. Froidevaux, C. (Eds.), Composition, Structure and Dynamics of the Lithosphere–Asthenosphere System. Am. Geophys. Union, Geodyn. Ser. 16, 111–123.

Patriat, P., Achache, J., 1984. Indian–Asia collision chronology has implications for crustal shortening and driving mechanisms of plates. Nature 311, 615–621.

Patzelt, A., Li, H., Wang, J., Appel, E., 1996. Paleomagnetism of Cretaceous to Tertiary sediments from southern Tibet: evidence for the extent of the northern margin of India prior to the collision with Eurasia. Tectonophysics 259, 259–284.

Prevot, R., Hatzfeld, D., Roecker, S.W., Molnar, P., 1980. Shallow earthquakes and active tectonics in eastern Afghanistan. J. Geophys. Res. 85, 1347–1357.

Ribe, N.M., 1989a. A continuum theory for lattice preferred orientation. Geophys. J. 97, 199–207.

Ribe, N.M., 1989b. Seismic anisotropy and mantle flow. J. Geophys. Res. 94, 4213–4223.

Roecker, S.W., 1982. Velocity structure of the Pamir–Hindu Kush region: Possible evidence of subducted crust. J. Geophys. Res. 87, 945–959.

Roecker, S.W., Soboleva, O.V., Nersevov, I.L., Lukk, A.A., Hatzfeld, D., Chatelain, J.L., Molnar, P., 1980. Seismicity and fault plane solutions of intermediate depth earthquakes in the Pamir–Hindu Kush region. J. Geophys. Res. 85, 1358–1364.

Russo, R.M., Silver, P.G., 1994a. Trench-parallel flow beneath the Nazca plate from seismic anisotropy. Science 263, 1105–1111.

Russo, R.M., Silver, P.G., 1994b. Shear-wave splitting in western Pacific subduction zones. Eos, Trans. Am. Geophys. Union 75, 449.

Russo, R.M., Silver, P.G., Franke, M., Ambeh, W.B., James, D.E., 1996a. Shear wave splitting in northeast Venezuela, Trinidad, and the eastern Caribbean. Phys. Earth Planet. Inter. 95, 251–275.

Russo, R.M., Lundgren, P.R., Margheriti, L., Giardini, D., D'Agostino, N., 1996b. Source-side shear wave splitting in the Mediterranean. Eos, Trans. Am. Geophys. Union 77.

Sandvol, E.A., Ni, J.F., Hearn, T.M., 1994. Seismic azimuthal anisotropy beneath the Pakistan Himalayas. Geophys. Res. Lett. 221, 1635–1638.

Searle, M.P. et al., 1987. The closing of Tethys and the tectonics of the Himalaya. Geol. Soc. Am. Bull. 98, 678–701.

Silver, P.G., 1996. Seismic anisotropy beneath the continents:

probing the depths of geology. Annu. Rev. Earth Planet. Sci. 24, 385–432.

Silver, P.G., Chan, W.W., 1991. Shear wave splitting and subcontinental mantle deformation. J. Geophys. Res. 96, 16429–16454.

Silver, P.G., Russo, R.M., 1995. Shear-wave splitting along the northern Australian plate boundary. Eos, Trans. Am. Geophys. Union 76, 413.

Silver, P.G., Savage, M.K., 1994. The interpretation of shear-wave splitting parameters in the presence of two anisotropic layers. Geophys. J. Int. 119, 949–963.

Tapponnier, P., Molnar, P., 1976. Slip-line field theory and large scale continental tectonics. Nature 264, 319–324.

Tapponnier, P., Mattauer, M., Proust, F., Cassaigneau, C., 1981. Mesozoic ophiolites, sutures and large-scale tectonic movements in Afghanistan. Earth Planet. Sci. Lett. 52, 355–371.

Treloar, P.J., Izatt, C.N., 1993. Tectonics of the Himalayan collision between the Indian Plate and the Afghan Block: a synthesis. In: Treloar, P.J., Searle, M.P. (Eds.), Himalayan Tectonics. Geol. Soc. London Spec. Publ. 16, 69–87.

Vinnik, L.P., Kind, R., 1993. Ellipticity of teleseismic S-particle motion. Geophys. J. Int. 113, 165–174.

Vinnik, L.P., Kind, R., Kosarev, G.L., Makeyeva, L.I., 1989a. Azimuthal anisotropy in the lithosphere from observations of long-period S-waves. Geophys. J. Int. 99, 549–559.

Vinnik, L.P., Farra, V., Romanowicz, B.A., 1989b. Azimuthal anisotropy in the Earth from observations of SKS at GEOSCOPE and NARS broadband stations. Bull. Seismol. Soc. Am. 79, 1542–1558.

Vinnik, L.P., Makeyeva, L.I., Usenko, A.Yu., 1992. Global patterns of azimuthal anisotropy and deformations in the continental mantle. Geophys. J. Int. 111, 433–447.

Wessel, P., Smith, W.H.F., 1991. Free software helps map and display data. Eos, Trans. Am. Geophys. Union 72, 445–446.

Wessel, P., Smith, W.H.F., 1995. New version of the Generic Mapping Tools released. Eos, Trans. Am. Geophys. Union 76, 329.

Yang, X., Fischer, K.M., Abers, G.A., 1995. Seismic anisotropy beneath the Shumagin Islands segment of the Aleutian–Alaska subduction zone. J. Geophys. Res. 100, 18165–18177.